

Cosmic ray confinement in the diffusion approximation

Andrew P. Snodin¹, Axel Brandenburg², Antony J. Mee¹, and Anvar Shukurov¹

¹*School of Mathematics and Statistics, University of Newcastle, Newcastle upon Tyne, NE1 7RU, UK*

²*NORDITA, Blegdamsvej 17, DK-2100 Copenhagen Ø, Denmark*

24 December 2018, Revision: 1.110

ABSTRACT

Confinement of cosmic rays by turbulent magnetic fields and the relation between magnetic and cosmic ray energy densities are investigated. Cosmic rays are assumed to diffuse preferentially along magnetic field lines. The implementation into a non-conservative high-order finite difference code is discussed. By solving an explicitly time-dependent equation for the cosmic ray energy flux, causality is restored and the maximum propagation speed is in this way limited to physically meaningful values. This is particularly useful in order to avoid numerical problems near magnetic X-points. It is shown that significant amounts of kinetic energy can be converted into cosmic ray energy via compression. Two processes for magnetic cosmic ray confinement are discussed: (i) enhancement of the residence time of cosmic rays in magnetic structures due to decreased perpendicular diffusion and (ii) the ability of the magnetic tension force to oppose perpendicular expansion of the cosmic ray density. Both processes are verified in the diffusion approximation, but their effect is shown to be weak. In turbulent flows the finite life time of magnetic structures decreases the prominence of cosmic ray confinement even further.

1 INTRODUCTION

The importance of cosmic rays for the dynamics of the interstellar medium (ISM) has long been recognized (Parker 1966; Berezhinskii et al. 1990). Spatial gradients of the cosmic ray pressure contribute significantly to the force balance in the ISM. If cosmic rays are confined within magnetic flux tubes, then the tendency toward pressure equilibrium reduces gas pressure within the tubes. Depending on the efficiency of cooling, either temperature or entropy will be approximately uniform across the tube, but in both cases density inside the tube will be decreased relative to the exterior, making the tube buoyant. This process is similar to magnetic buoyancy. In the sun, magnetic buoyancy drives magnetic flux tubes to the surface to form bipolar regions. In galaxies, magnetic buoyancy is believed to be strongly assisted by cosmic rays. Therefore, cosmic rays facilitate disc-halo connections in spiral galaxies by enhancing buoyancy of the magnetized interstellar gas.

The effects of cosmic-ray driven buoyancy are believed to be important for the operation of the galactic dynamo (Parker 1992; Moss et al. 1999). This can significantly speed up the growth of the field and maintain strong field amplification and regeneration, especially in the nonlinear regime (Hanasz et al. 2004). In many studies of the Parker instability and recent simulations of the galactic dynamo, cosmic rays have been included using the diffusion approximation. However, it remains unclear to what extent in these simulations cosmic rays were confined by the magnetic field, and whether any equipartition between cosmic rays and the magnetic field was maintained.

Energy equipartition (or pressure balance) between cos-

mic rays and magnetic fields is one of key paradigms of radio astronomy, where it provides the most often used method to estimate magnetic field strength from synchrotron intensity. However, the physical basis of this concept remains elusive, and only qualitative arguments related to cosmic ray confinement by magnetic fields are used to justify this concept. However, the spatial distribution of cosmic rays cannot precisely follow that of magnetic field strength, at least because cosmic rays have large diffusivity, so that they diffuse along magnetic field lines over 0.5 kpc in 10^6 years (for a parallel diffusivity of $4 \times 10^{28} \text{ cm}^2 \text{ s}^{-1}$). Furthermore, the idea of overall (statistical) pressure balance in the ISM would be more difficult to maintain if both magnetic and cosmic ray pressures are enhanced or reduced at the same positions simultaneously. Recent arguments of Padoan & Scalo (2005) suggest that, if the streaming velocity of cosmic rays is proportional to the Alfvén speed (Felice & Kulsrud 2001; Farmer & Goldreich 2004, and references therein), the local cosmic ray density is independent of the local magnetic field strength, but rather scales with the square root of the (ionized) gas density. Indeed, if both the magnetic flux and the cosmic ray flux are conserved, $BS = \text{const}$ and $n_c US = \text{const}$ (where B is the magnetic field strength, S is the area within a fluid contour, n_c is the number density of cosmic rays and U is their streaming velocity), one obtains $n_c U/B = \text{const}$, which yields $n_c \propto n_g^{1/2}$, given that $U \propto V_A \propto B n_g^{-1/2}$, with n_g the gas number density and V_A the Alfvén speed. We note that these arguments are of a more general character than the diffusion approximation.

The purpose of the present paper is to assess the degree of cosmic ray confinement within the framework of the dif-

fusion approximation. In particular we want to know which process is mainly responsible for limiting the cosmic rays energy density, and what is the relation of cosmic ray energy density with the magnetic field. Is there local equipartition, or is there only global equipartition on the scale of the galaxy? Finally, we are interested in studying those effects in the ISM dynamics that only arise in the presence of cosmic rays. We begin with the governing equations and discuss issues that arise in connection with the numerical implementation of cosmic ray diffusion along magnetic field lines.

2 METHOD

2.1 Basic equations

The hydromagnetic equations, supplemented by the cosmic ray advection-diffusion equation and the cosmic ray pressure in the momentum equation, are

$$\frac{\partial \rho}{\partial t} + \nabla \cdot (\rho \mathbf{u}) = 0, \quad (1)$$

$$\frac{\partial e_c}{\partial t} + \nabla \cdot (e_c \mathbf{u}) + p_c \nabla \cdot \mathbf{u} = D_c + Q_c, \quad (2)$$

$$\frac{\partial e_g}{\partial t} + \nabla \cdot (e_g \mathbf{u}) + p_g \nabla \cdot \mathbf{u} = D_g + Q_k + Q_m, \quad (3)$$

$$\frac{\partial \rho \mathbf{u}}{\partial t} + \nabla \cdot (\rho \mathbf{u} \mathbf{u}) + \nabla (p_g + p_c) = \mathbf{J} \times \mathbf{B} + \mathbf{f} + \mathbf{F}, \quad (4)$$

$$\frac{\partial \mathbf{B}}{\partial t} = \nabla \times (\mathbf{u} \times \mathbf{B} - \eta \mu_0 \mathbf{J}), \quad (5)$$

where ρ , \mathbf{u} and p_g are the gas density, velocity and pressure; e_c and p_c are the cosmic ray energy density and pressure, \mathbf{B} is the magnetic field, $\mathbf{J} = \nabla \times \mathbf{B} / \mu_0$ is the electric current density, $D_g = \nabla \cdot (K \nabla T)$ is the thermal diffusion term (treated here isotropically; thermal diffusion is negligible in galaxies, but weak diffusion is necessary for numerical reasons). Further, T is the temperature which is related to the internal energy density (per unit volume), e_g , via $e_g = \rho c_v T$, and D_c is the divergence of the diffusive cosmic ray energy flux taken with the opposite sign, i.e.

$$D_c = -\nabla \cdot \mathcal{F}_c. \quad (6)$$

The usual approach is to treat this term as Fickian diffusion, and to assume that the flux is proportional to the instantaneous gradient of the cosmic ray energy density, i.e.

$$\mathcal{F}_{ci} = -K_{ij} \nabla_j e_c \quad (\text{Fickian diffusion}), \quad (7)$$

where K_{ij} is an anisotropic diffusion tensor. In its simplest form this can be written as

$$K_{ij} = K_{\perp} \delta_{ij} + (K_{\parallel} - K_{\perp}) \hat{B}_i \hat{B}_j, \quad (8)$$

where $\hat{\mathbf{B}} = \mathbf{B} / |\mathbf{B}|$ is the field-aligned unit vector (e.g. Berezhinskii et al. 1990; Hanasz & Lesch 2003). Here, K_{\parallel} and K_{\perp} are the cosmic ray diffusion coefficients along and perpendicular to the field, respectively.

We assume ideal-gas equations of state for both the cosmic rays and the gas, i.e. $p_c = (\gamma_c - 1)e_c$ and $p_g = (\gamma_g - 1)e_g$, where γ_c and γ_g are the ratios of the total number of degrees of freedom to the number of translational degrees of freedom for the cosmic rays and the gas. Unless noted otherwise we assume $\gamma_c = 4/3$ and $\gamma_g = 5/3$. Other choices

include $\gamma_c = 5/3$ and $\gamma_c = 14/9$ (e.g. Ryu et al. 2003, and references therein).

The system can be driven by an external force \mathbf{f} ; $Q_k = 2\rho \nu \mathbf{S}^2$ and $Q_m = \eta \mu_0 \mathbf{J}^2$ denote the viscous and Joule heating, and Q_c is a cosmic ray energy source.

2.2 Non-Fickian diffusion

Estimations of the field-aligned diffusion coefficient give rather large values. Typical values are of the order $10^{28} \text{ cm}^2 \text{ s}^{-1}$ (e.g. Strong & Moskalenko 1998). This diffusion coefficient is closely related to our K_{\parallel} , which is actually an energy-weighted diffusion coefficient (see, for example, Ryu et al. 2003). Here we use the two synonymously. Such large values would severely limit numerical modelling since a large diffusivity requires that the computational time step is small to ensure numerical stability (e.g., Hanasz & Lesch 2003 reduce K_{\parallel} by a factor of 10 to make the system tractable numerically). This problem could be circumvented by employing an implicit numerical scheme. However, this does not resolve the fundamental difficulty of the Fickian diffusion where the (weak) tail of the diffusing quantity spreads at infinite speed. In the context of cosmic ray propagation, one would expect the propagation speed to be not much larger than the Alfvén speed.

There is another related problem. If we use the product rule and write $D_c = \nabla_i (K_{ij} \nabla_j e_c)$ in the form

$$D_c = -\mathbf{U}_c \cdot \nabla e_c + K_{ij} \partial_i \partial_j e_c, \quad (9)$$

we see that $U_{ci} = -\partial K_{ij} / \partial x_j$ plays the role of a velocity dragging cosmic rays along curved field lines. This term is proportional to the divergence of the dyadic product of unit vectors, $\nabla \cdot (\hat{\mathbf{B}} \hat{\mathbf{B}})$. Near magnetic stagnation points, this term is singular.

A simple magnetic field configuration leading to the singular behaviour of $\nabla \cdot (\hat{\mathbf{B}} \hat{\mathbf{B}})$, and hence to a singularity of $|U_c|$, is given by $\mathbf{B} = (x, -y, 0)^T$. This leads to

$$\nabla \cdot (\hat{\mathbf{B}} \hat{\mathbf{B}}) = \frac{1}{r^4} \begin{pmatrix} (3y^2 - x^2)x \\ (3x^2 - y^2)y \\ 0 \end{pmatrix}, \quad (10)$$

where $r^2 = x^2 + y^2$. This expression diverges at the origin and leads to infinite propagation speed which would, technically speaking, limit to zero the length of the timestep of an explicit timestepping scheme. In spite of this singularity, the cosmic ray energy density must stay finite. In fact, one can show that, in a closed or periodic domain, the maximum cosmic ray energy density, $\max(e_c)$, can only decrease with time (see Appendix A). Of course, this is a well-known general property of the diffusion operator; here we provide explicit derivation of this result for the form of the diffusion tensor specific for cosmic rays. A physically appealing way of limiting the maximum propagation speed is to restore an explicit time dependence in the equation for the cosmic ray flux, and to replace Eq. (7) by

$$\frac{\partial \mathcal{F}_{ci}}{\partial t} = -\tilde{K}_{ij} \nabla_j e_c - \frac{\mathcal{F}_{ci}}{\tau} \quad (\text{non-Fickian diffusion}), \quad (11)$$

where $K_{ij} = \tau \tilde{K}_{ij}$ would be the original diffusion tensor of Eq. (8), if the time derivative were negligible. Moreover, in analogy with Eq. (8) we write

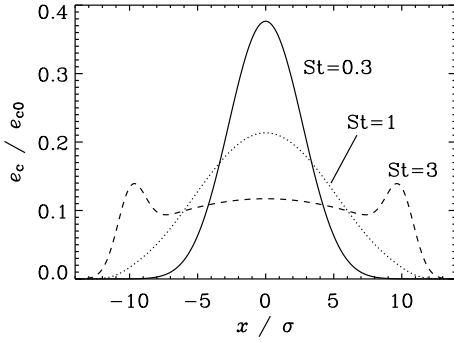


Figure 1. The spread of an initial Gaussian distribution of cosmic ray energy density (of a half-width σ): the distribution at a time $t = 1$ is shown for three different values of the Strouhal number St . Note that the behaviour of the solution becomes more wave-like as St increases.

$$\tilde{K}_{ij} = \tilde{K}_{\perp} \delta_{ij} + (\tilde{K}_{\parallel} - \tilde{K}_{\perp}) \hat{B}_i \hat{B}_j. \quad (12)$$

This type of non-Fickian diffusion emerges quite naturally also in turbulent diffusion of passive scalars (Blackman & Field 2003) and has been confirmed in direct simulations (Brandenburg et al. 2004). Note that on long enough time scales, or for sufficiently small values of τ , the non-Fickian diffusion agrees with the Fickian diffusion. Quantitatively, this is controlled by the nondimensional parameter

$$St = \tilde{K}_{\parallel}^{-1/2} \tau / \ell, \quad (13)$$

where ℓ is the typical length scale of the initial structure. In the context of turbulent diffusion, this nondimensional parameter is sometimes referred to as the Strouhal number (Landau & Lifshitz 1987; Krause & Rädler 1980). In Fig. 1 we illustrate a one-dimensional spread of an initial Gaussian distribution of cosmic rays, $e_c = \exp(-\frac{1}{2}x^2/\ell^2)$ after $t = \tau$ for three values of St . For small values of St , the solution evolves similarly to that of the diffusion equation (solid and dotted lines in Fig. 1). However, for large values of St , the distribution of cosmic rays develops two local maxima of e_c that propagate outwards as shown with dashed line, a typical wave-like behaviour. In the limiting case of very large values of St the governing equation reduces to the wave equation, and for $St \rightarrow 0$ the classical diffusion is recovered. For finite values of St , the resulting equation for e_c is known as the telegraph equation.

The extra time derivative in the non-Fickian diffusion formulation is formally equivalent to the Faraday displacement current in electrodynamics. In simulations of hydro-magnetic flows at low density, where the Alfvén speed can be very large, the displacement current is sometimes included with an artificially lowered value of the speed of light. This automatically limits the Alfvén speed to numerically acceptable values.

A comment regarding centred finite difference schemes is here in order. In the steady state, the discretization of the cosmic ray diffusion formalism in the form given by Eqs (6) and (11) corresponds essentially to a conservative formulation of the diffusion term. (A non-conservative formulation involving a direct discretization of ∇^2 is not possible here,

because two first order derivatives occur in two separate equations.) As is well known, the discretization of the diffusion term on a centred non-staggered mesh means that structures at the mesh scale cannot be diffused (the discretization error for first derivatives becomes infinite). Therefore we have to restore an explicit but small additive Fickian diffusion term in the cosmic ray energy equation. We refer to the corresponding (isotropic) diffusion coefficient as K_{Fick} , and it will be chosen to be comparable to or less than the value of the viscosity or the magnetic diffusivity.

In the following we use the PENCIL CODE,¹ which is a non-conservative high-order finite-difference code (sixth order in space and third order in time) for solving the compressible hydromagnetic equations. The non-Fickian diffusion formulation is invoked by using the `cosmicrayflux` module. Whenever possible we display the results in non-dimensional form, normalizing in terms of physically relevant quantities. In all other cases we display the results in code units, which means that velocities are given in units of the sound speed c_s , length is given in units of k_1^{-1} , density is given in units of the average density ρ_0 , and magnetic field is given in units of $\sqrt{\mu_0 \rho_0} c_s$. The units of all other quantities can be worked out from this. For example, the unit of Q_c is $\rho_0 c_s^3 k_1$. For the interstellar medium with $\rho_0 = 10^{-24} \text{ g cm}^{-3}$, $c_s = 10 \text{ km s}^{-1}$, and $k_1 = 2\pi/100 \text{ pc}$, the unit of the heating rate is $3 \times 10^{-26} \text{ erg cm}^{-3} \text{ s}^{-1}$, which is about ten times less than the rate of energy injection by supernovae in the galactic disc of about $2 \times 10^{-25} \text{ erg cm}^{-3} \text{ s}^{-1}$. The latter value is consistent with the values used by Korpi et al. (1999).

2.3 Cosmic ray diffusion near a magnetic X-point

We test the field-aligned diffusion procedure by simulating in two dimensions a magnetic field configuration similar to the X-point discussed in Sect. 2.2. In order to be able to impose normal-field boundary conditions, $\hat{n} \times \mathbf{B} = 0$ at the domain boundaries, we modify the field to $\mathbf{B} = (\sin k_1 x, -\sin k_1 y, 0)^T$, where k_1 is the smallest wavenumber in a periodic domain. So, for $k_1 = 1$ we consider the domain $-\pi < (x, y) < \pi$. The initial distribution of the cosmic ray energy density is $e_c = x$, which has a constant gradient and therefore, with Fickian diffusion, $D_c = \nabla \cdot (\hat{\mathbf{B}} \hat{\mathbf{B}})$ would have a singularity initially. However, in the non-Fickian approach D_c is not calculated as in Eq. (9), which resolves this problem. The evolution of e_c is shown in Fig. 2 together with vectors showing the magnetic field. Note that the gradient of e_c is small in the neighbourhood of the singularity of $\nabla \cdot (\hat{\mathbf{B}} \hat{\mathbf{B}})$ at the origin, so the singularity that multiplies ∇e_c has no effect on e_c , as desired. In the case of the Fickian diffusion, the same final solution would have been obtained, but the initial reduction of the gradient in e_c would have involved an infinitely fast advection speed U_c . In the non-Fickian approach, the maximum propagation speed is $\tilde{K}_{\parallel}^{-1/2}$, thereby alleviating the numerical timestep problem.

Another example of field-aligned diffusion is shown in Fig. 3, where the magnetic field is given by $\mathbf{B} = \mathbf{B}_0 + \nabla \times \mathbf{A}$ with $\mathbf{B}_0 = 0.1 \hat{x}$ and $\mathbf{A} = 0.1 \hat{z} \cos(k_x x) \cos(k_y y)$ with $k_x = 4k_1$ and $k_y = k_1$. Again, this magnetic field is kept fixed in time, so this calculation is purely kinematic. The

¹ <http://www.nordita.dk/software/pencil-code>

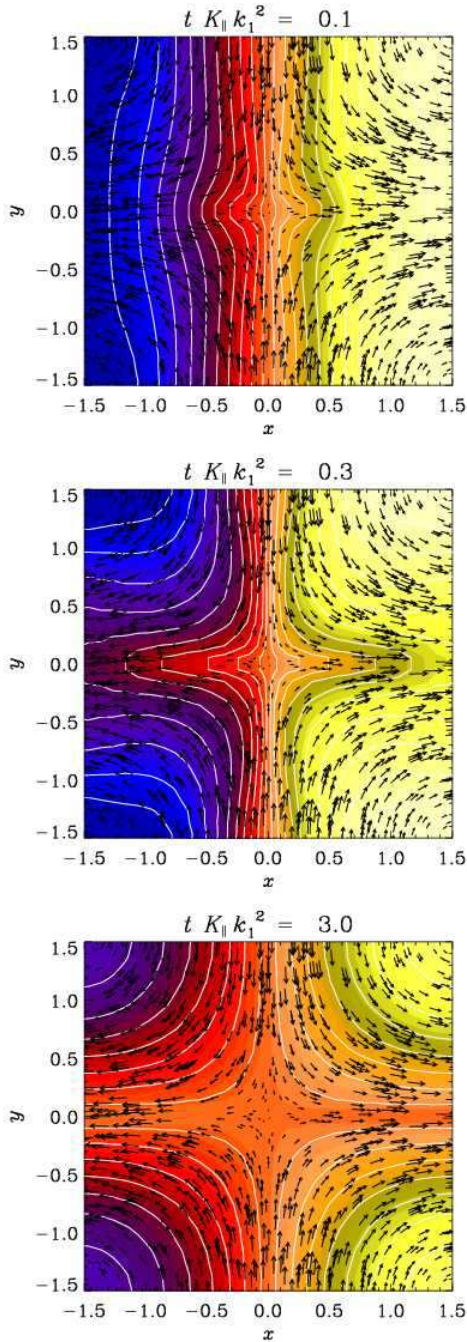


Figure 2. Evolution of the cosmic ray energy density near a magnetic X-point: snapshots of e_c (shown as contours and shades of grey/colour) for field-aligned diffusion along a fixed magnetic field $\mathbf{B} = (\sin k_1 x, -\sin k_1 y, 0)^T$ (shown as vectors) displayed for three times indicated at the top of each frame.

initial profile of $e_c \propto \exp(-r^2/2\sigma^2)$, with $r^2 = x^2 + y^2$, is a two-dimensional Gaussian of a half-width of $\sigma = 0.07$, positioned at $x = 0$ and $y = -0.5$. We confirm that our implementation of cosmic ray diffusion allows us to model reliably rather complicated magnetic configurations. The lower panel of Fig. 3 confirms that, for large values of the Strouhal number, the wave nature of the telegraph equation manifests

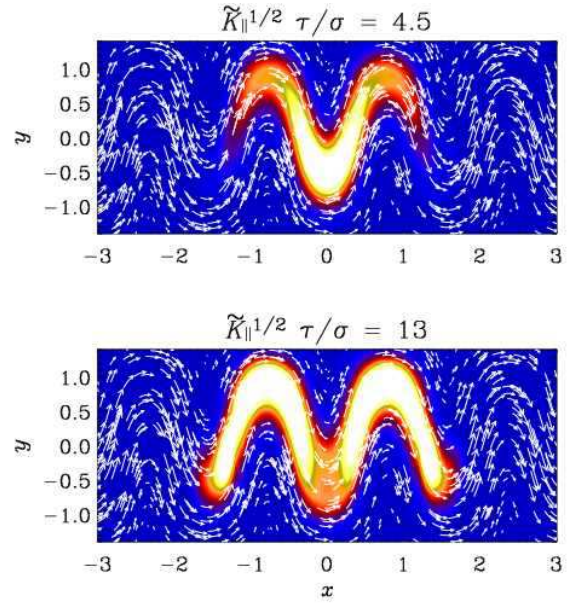


Figure 3. Magnetic field vectors together with a grey/colour scale representation of e_c in a kinematic calculation with 128^2 meshpoints, for different values of $K_{\parallel}^{1/2} \tau / \sigma$, with $\tilde{K}_{\perp} = 0$, $\tilde{K}_{\parallel} = 10^{-1}$, and $K_{\text{Pick}} = 10^{-3}$, at time $t/\tau = 1$ for two different values of τ ($=1$ and 3 , respectively). (Only part of the computational domain in the y direction is shown.)

itself and e_c develops two waves propagating away from the initial maximum (similar to the dashed line in Fig. 1).

3 ENERGY

3.1 General considerations

In a closed domain, mass is conserved, i.e. $\langle \rho \rangle \equiv \rho_0 = 1$, where angular brackets denote volume averaging. Then the hydromagnetic equations coupled with cosmic ray dynamics lead to the following set of equations for the cosmic ray energy $E_c = \langle e_c \rangle$, the gas energy $E_g = \langle e_g \rangle$, the kinetic energy $E_k = \langle \frac{1}{2} \rho \mathbf{u}^2 \rangle$, and magnetic energy $E_m = \langle \mathbf{B}^2 \rangle / 2\mu_0$,

$$\frac{dE_c}{dt} = -W_c + \tilde{Q}_c, \quad (14)$$

$$\frac{dE_g}{dt} = -W_g + \tilde{Q}_k + \tilde{Q}_m, \quad (15)$$

$$\frac{dE_k}{dt} = W_c + W_g + W_m + W_f - \tilde{Q}_k, \quad (16)$$

$$\frac{dE_m}{dt} = -W_m - \tilde{Q}_m. \quad (17)$$

Here, all the energies are referred to the unit volume. The terms $W_c = \langle p_c \nabla \cdot \mathbf{u} \rangle$, $W_g = \langle p_g \nabla \cdot \mathbf{u} \rangle$, $W_m = \langle \mathbf{u} \cdot (\mathbf{J} \times \mathbf{B}) \rangle$, and $W_f = \langle \mathbf{u} \cdot \mathbf{f} \rangle$ denote work done against cosmic ray pressure, gas pressure, Lorentz force, and the external forcing, respectively. Terms responsible for viscous and Joule heating and the cosmic ray energy source are simply given by the volume integrated terms in the original equations, e.g. $\tilde{Q} = \langle Q \rangle$. Equations (14)–(17) imply that the total energy, $E_{\text{tot}} = E_c + E_g + E_k + E_m$, satisfies the simple conservation law

$$\frac{dE_{\text{tot}}}{dt} = \tilde{Q}_c + W_f. \quad (18)$$

Thus, unless there is optically thin radiative cooling, the only sources of energy are the injection of cosmic ray energy and the external forcing of the turbulence. In the following section we demonstrate how E_c can be enhanced by the conversion of kinetic energy.

3.2 Compressional enhancement of cosmic ray energy

We assume $\tilde{Q}_c = W_f = 0$ and that there is initially kinetic energy that is later redistributed among gas and cosmic rays. We investigate, using a simple one-dimensional model ($\partial/\partial y = \partial/\partial z = 0$), how much energy can be converted into cosmic ray energy via the W_c term responsible for work done against cosmic ray pressure. As an initial condition, we use a sinusoidal perturbation of u_x and $\ln \rho$ with unit amplitude and $E_c = E_{c0} = 1$, $E_g = 1.8$, and $E_k = 0.21$. The evolution of velocity, cosmic ray and gas energies, as well as the entropy of the gas are shown in Fig. 4. Here the entropy s is defined as $s = c_v \ln(c_s^2/\rho g^{\gamma-1})$, where $c_s^2 = \gamma(\gamma - 1)e_g$ is the squared sound speed of the gas. It turns out that in this case about 78% of the kinetic energy is transformed into cosmic ray energy and only 22% into thermal energy. This result is however sensitive to the phase shift between density and velocity: if the density is initially uniform (keeping all other parameters unchanged), the fractional energy going into cosmic rays is only 23% and 77% go into thermal energy.

These results demonstrate that, at least in principle, a sizeable fraction of the kinetic energy can be converted into cosmic ray energy. Similar results have been found earlier (see, e.g., Drury & Völk 1981; Jun et al. 1994). In particular Kang & Jones (1990) showed that the efficiency of conversion varies strongly with γ_c . However, the conversion of kinetic energy into cosmic ray energy requires a background of cosmic ray energy. Decreasing E_c from 1 to 0.1 lowers the fraction of compressionally produced cosmic ray energy density from 78% to 21%. In contrast to dynamo theory where a weak seed magnetic field is sufficient to produce equipartition magnetic fields (albeit only in three dimensions), there is no such mechanism for the cosmic ray energy. This is related to the anti-dynamo theorem for scalar fields (Krause 1972). However, for three-dimensional compressible flows an exponential dynamo-like amplification of a passive scalar is in principle possible if the passive scalar is described by inertial particles (Elperin et al. 1996). Such a mechanism can work because inertial particles do not feel a pressure gradient. This can lead to particle accumulation in temperature minima (Elperin et al. 1997) and in vortices (Barge & Sommeria 1995; Hodgson & Brandenburg 1998; Johansen et al. 2004). However, in this paper cosmic ray particles are treated as non-inertial particles.

4 CONFINEMENT EXPERIMENTS

Cosmic rays can only be dynamically important if their distribution is nonuniform, so that cosmic ray pressure gradient does not vanish. As discussed above, one may a priori expect the cosmic ray energy density to be related to the magnetic

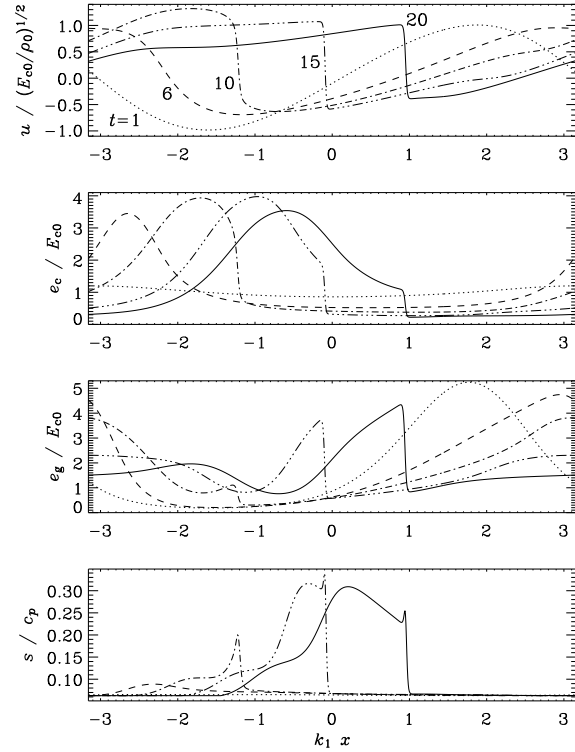


Figure 4. Velocity, cosmic ray and gas energy densities, and entropy in an experiment with a nonlinear sound wave that piles up to a shock ($\gamma_c = 5/3$). Note the significant conversion of kinetic energy into cosmic ray energy. The conversion into gas energy is comparatively small even though there is noticeable entropy enhancement due to the shock. The different line types and are explained in the first panel. Time is given in units of $k_1^{-1}(E_{c0}/\rho_0)^{-1/2}$.

field strength. However, it is not immediately clear how such a relation can arise, at least in the diffusion approximation for cosmic rays. In the following we discuss two mechanisms that could contribute to a magnetic modulation of the cosmic ray energy density, and perhaps even to their preferred confinement into magnetic flux tubes.

4.1 Effect of cosmic ray pressure

Cosmic rays can in principle be confined by the magnetic field if the flux tubes can act as magnetic bottles trapping electrically charged cosmic ray particles. The particles can plausibly be confined only if the energy of the cosmic ray particles does not exceed the energy of the magnetic field. This would provide a natural mechanism for producing equipartition between cosmic rays and the magnetic field. Particles outside the magnetic flux tube would remain unconfined and can expand freely. In the diffusion approximation, there are no particles that could spiral along field lines and hence magnetic bottles cannot exist. Nevertheless, there is a related dynamical effect where confinement is based on the fact that strong fields can more easily withstand deformation through gradients of the cosmic ray pressure.

This feature can be simulated in two dimensions in a doubly periodic domain $-\pi < (x, y) < \pi$, using $k_1 = 1$. The results are illustrated in Fig. 5, where we have a magnetic

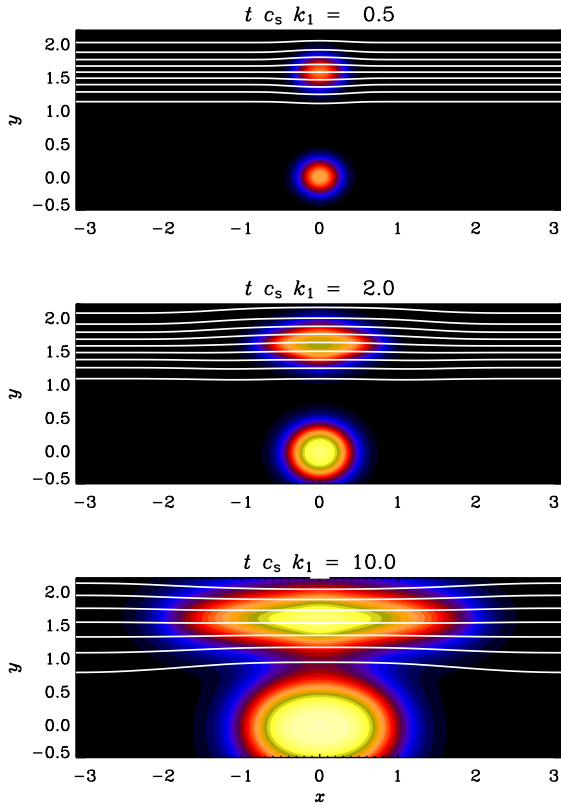


Figure 5. Cosmic ray energy density at different times. There are two cosmic ray sources, one inside a magnetic flux tube and the other one outside. Here, $R = 0.13$ and $\tilde{Q}_c = 10$. Note the field-aligned diffusion inside the magnetic structure and the more isotropic diffusion where the field is weak.

tube in $1 < y < 2$ with its axis along the x direction. We have implemented two local cosmic ray sources with

$$\tilde{Q}_c = \tilde{Q}_{c0} \sum_{i=1}^2 \exp \left\{ -\frac{1}{2} [x^2 + (y - y_i)^2] / R^2 \right\}, \quad (19)$$

i.e., both located on the x axis but centred at $y_1 = 0$ and $y_2 = \pi/2$. In this experiment, cosmic ray diffusion is negligible ($\tilde{K}_{\parallel} = \tilde{K}_{\perp} = 0$ and $K_{\text{Fick}} = 0.01$) as we intend to explore the effects of cosmic ray pressure alone. The overpressure due to cosmic rays will drive expansion, resisted by the magnetic field. As expected, expansion proceeds nearly isotropically outside the magnetic structure, and the cosmic ray energy density is channelled preferentially along field lines inside the tube. At the end of the run, the aspect ratio of the cosmic ray distribution is about 2 inside the tube. However, a more intense injection of cosmic rays does not seem to lead to much stronger anisotropy of the cosmic ray distribution. For values of \tilde{Q}_c significantly larger than about 10, gas density decreases strongly as to maintain pressure equilibrium, and this limits expansion driven by cosmic rays. Smaller values of \tilde{Q}_c lead to even smaller aspect ratios.

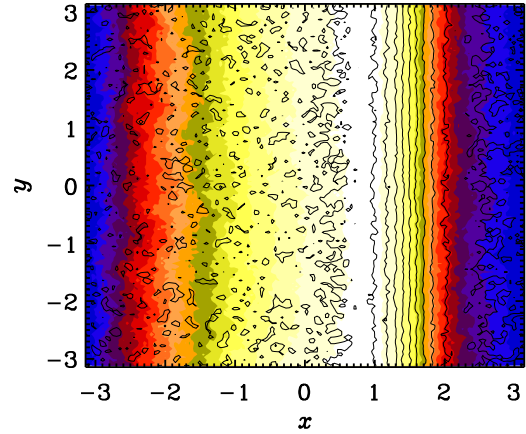


Figure 6. Cosmic ray energy density (colour/grey scale coded, with darker/blue shades corresponding to smaller values) together with magnetic field lines in a two-dimensional simulation with a frozen magnetic flux tube centred around $x = 1.5$ and a fixed random field outside. The cosmic ray density appears rather symmetrically arranged about $x = 0$, even though the flux tube is clearly away from the middle.

4.2 Magnetic flux tube embedded in a random field

Given that the cosmic ray pressure is relatively inefficient in dispersing the cosmic ray energy density (Sect. 4.1), we must look for alternatives in order to explain confinement of cosmic rays in the diffusion approximation. One possibility is that outside the confining tubes the field is not only weak, but also randomly oriented, so cosmic rays propagating along field lines would have on average a $1/3$ chance in rapidly diffusing perpendicular to the large-scale magnetic tube. In addition, turbulent magnetic field can facilitate cosmic ray diffusion by destroying the compound diffusion effect (Kóta & Jokipii 2000, and references therein) due to the exponential local divergence of magnetic lines.

Although the experiments with fully periodic boxes can show a trend toward confinement, they will never demonstrate net confinement: if particles are injected outside the flux tube they will be confined to the finite volume outside the tube by the periodic boundary conditions. We therefore need to allow for particles to be lost through the x boundaries, as will be done in the present section. At $x = \pm\pi$, we therefore assume a zero value for the cosmic ray energy density, $e_c = 0$, but zero normal derivative for the density and energy density of the gas, i.e. $\partial\rho/\partial x = \partial e_g/\partial x = 0$. This implies that cosmic rays will be lost from the domain (as desired), but not the gas. In the y direction we still use periodic boundary conditions.

We consider a two-dimensional system with magnetic field confined to a flux tube aligned with the y axis as shown in Fig. 6 where the tube is centred at $x = 1.5$. The magnetic field strength has a Gaussian profile across the tube with a width of 0.5. The magnetic field has a regular part directed along the y axis, \mathbf{B}_0 and an isotropic random part $\delta\mathbf{B}$, with a ratio of strengths $\delta B/\max(B_0) = 1$ at $x = 1.5$. The random magnetic field is implemented in terms of magnetic vector potential given as white noise with Gaus-

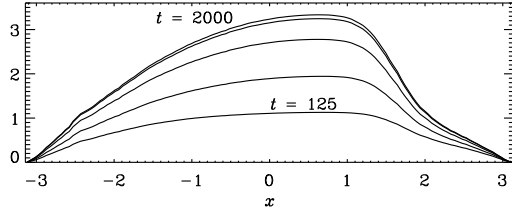


Figure 7. Cosmic ray energy density averaged in the y direction for times 125×2^n with $n = 0, \dots, 4$. The tube is located at $x = 1.5$, which leads to an asymmetric distribution of cosmic ray energy density, and hence to a clear departure from the otherwise parabolic equilibrium profile.

sian probability density, which implies a k^4 power spectrum for the magnetic energy. In order to keep the relative importance of random and regular fields, we assume the magnetic field frozen in time. We also assume zero velocity for all times, so we just advance Eqs (2) and (11) in time, using Eq. (6). Cosmic rays are injected at constant rate across the domain, $Q_c = \text{const}$.

In Fig. 6 we show the result of such a calculation; it is notable that the cosmic ray energy density is concentrated around the middle of the domain in x as might be expected given the symmetric boundary conditions imposed at $|x| = \pi$. However, the distribution of cosmic rays in x is asymmetric. This asymmetry can be seen more clearly in Fig. 7 which shows the cosmic ray energy density *averaged* in the y direction for several different times. Note however that the steady state is only attained after very long times. (Here, $\tau = 3$ and $\tilde{K}_{\parallel} = 0.1$, so $t = 2000$ corresponds to $t\tilde{K}_{\parallel}k_1^2 = 600$.) Nevertheless, the $e_c(x)$ profile appears roughly similar at early and late times.

In order to understand this behaviour let us consider a simple one-dimensional model, where we have large perpendicular diffusion (from the random field) outside the tube and small perpendicular diffusion inside the tube. Here, the field points in the y direction, but the only variations are perpendicular to the field, i.e. in the x direction. We therefore consider a profile of $K_{\perp}(x)$ that is, say, ten times smaller in the tube than outside. For a uniform injection of cosmic rays, the one-dimensional steady-state cosmic ray concentration is governed by the equation

$$0 = \tilde{Q}_c + \frac{d}{dx} \left(K_{\perp} \frac{de_c}{dx} \right). \quad (20)$$

For constant diffusivity, $K_{\perp} = \text{const}$, the equilibrium cosmic ray profile is given by $e_c = \frac{1}{2}(L_x^2 - x^2)\tilde{Q}_c/K_{\perp}$, where $L_x = 2\pi$ is the extent of the domain in the x direction. If the perpendicular diffusivity is locally decreased in the tube, the cosmic ray concentration in the tube tends to be enhanced. Examples of solutions of Eq. (20) are shown in Fig. 8 for different profiles of $K_{\perp}(x)$.

The flux tube in the simulation shown in Fig. 6 and Fig. 7 is initially located at $x = 1.5$, which leads to an asymmetric distribution of cosmic ray energy density, and hence to a clear departure from the otherwise parabolic equilibrium profile (which would be symmetric). We conclude that the uppermost curve of Fig. 7 (latest time, near to equilibrium) is very similar to the model results shown in the

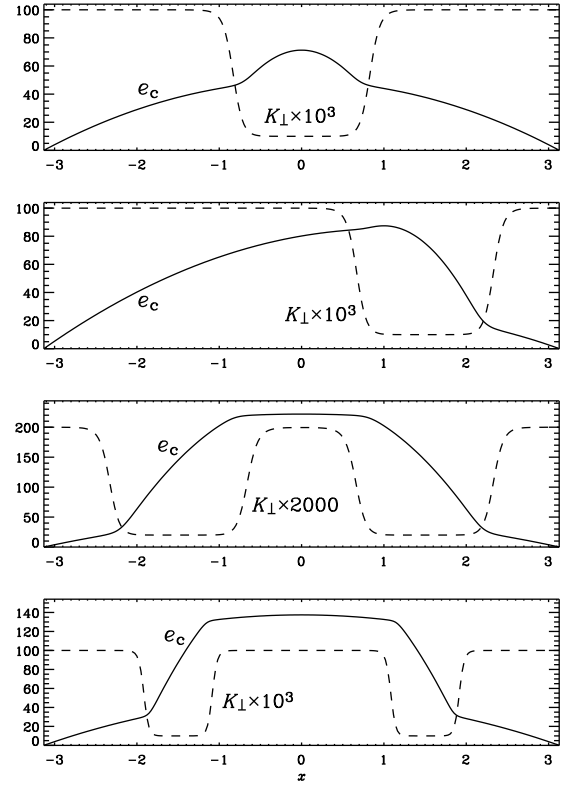


Figure 8. Solution of the one-dimensional diffusion equation (solid line), see Eq. (20), for a model profile (shown as in dashed). Note that, although the cosmic ray energy density is locally enhanced as a result of reduced losses from the flux tube, the main signature of this process is the marked asymmetry, which depends on the distance from the open boundaries.

second panel of Fig. 8, where the tube also goes through $x = 1.5$.

4.3 Turbulence simulation

Three-dimensional turbulence at large magnetic Reynolds numbers is capable of dynamo action, and the dynamo-generated magnetic field organizes itself into random flux tubes or sheets (e.g. Zeldovich et al. 1990; Brandenburg et al. 1995). Most studies of cosmic ray dynamics neglect the specific features of the dynamo-generated magnetic fields. Therefore, we provide here a preliminary discussion of cosmic ray confinement in a magnetic field generated by a turbulent flow of electrically conducting fluid. The turbulence in our simulations is driven helically by a forcing function in the Navier-Stokes equation, just like in the simulations of Brandenburg (2001) and Brandenburg & Dobler (2001). In the latter paper the same boundary conditions in the x direction were used as in Sects 4.2 and 4.3. The forcing function is given in Appendix B and its (nondimensional) amplitude is chosen to be $f_0 = 0.05$, which implies an rms Mach number of about 0.2.

The forcing wavenumber is chosen to be $k_f = 1.5 k_1$. This value is quite close to the wavenumber of the box, $k_1 = 2\pi/L_x$, so there is not enough scale separation to allow for the inverse cascade of magnetic helicity to develop

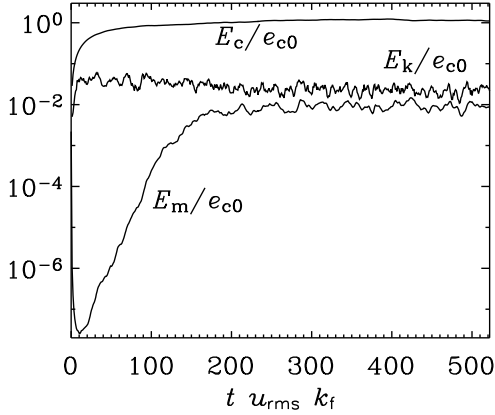


Figure 9. Time series of magnetic, kinetic and cosmic ray energies in a fully three-dimensional dynamo simulation. Here, time is given in turnover times $(u_{\text{rms}} k_f)^{-1}$, and $e_{c0} = L_x^2 \tilde{Q}_c / K_{\parallel}$ is used to normalize energies per unit volume. The thermal energy of the gas is constant with $E_g/e_{c0} \approx 0.7$.

(Haugen et al. 2004). Nevertheless, the presence of helicity can yield a lower threshold of the magnetic Reynolds number, $R_m \equiv u_{\text{rms}}/(\eta k_f)$, for the onset of dynamo action. However, because of the presence of boundaries in the x direction, and also because of the small amount of scale separation, the critical value of R_m is still around 30. In present case we have $R_m \approx 100$, which is about 3 times supercritical. The kinematic growth rate of the magnetic field is about $0.06 u_{\text{rms}} k_f$. The time evolution of the magnetic energy is shown in Fig. 9 and compared with kinetic and cosmic ray energies. Here we have chosen $\tilde{Q}_c = 0.01$, which yields $E_c \approx 1$ in our units. The other parameters of the simulation presented here are $\tilde{K}_{\perp} = 0$, $\tilde{K}_{\parallel} = 0.3$, $K_{\text{Fick}} = 5 \times 10^{-3}$, $\tau = 0.3$, $\eta = 10^{-3}$, $\nu = 2 \times 10^{-3}$. Our value of \tilde{K}_{\parallel} is chosen to be close to the maximum squared Alfvén velocity. For the chosen value of τ , we have $\text{St} \approx 1$ for the thin tube-like structures with a gaussian width of $\ell = 0.2$ in the current simulation; see Eq. (13). Using $K_{\parallel} = \tau \tilde{K}_{\parallel}$, this corresponds to a cosmic ray diffusivity of $\tilde{K}_{\parallel} \approx \nu_t$, where we have used $\nu_t \approx 0.7 u_{\text{rms}}/k_f$ as an estimate of the effective turbulent viscosity (Yousef et al. 2003). The adopted value of τ , and hence of K_{\parallel} , is rather near the bottom of the range of expected values. Up to ten times larger values of τ may still be reasonable, but then the effective values of St would exceed unity for the small tube-like structures, so the cosmic rays would not diffuse, but they would propagate more nearly ballistically.

In Fig. 10 we show an arbitrarily chosen cross-section of the cosmic ray energy density and magnetic field vectors from the three-dimensional dynamo simulation of Fig. 9 at $t = 510/(u_{\text{rms}} k_f)$. One sees clearly that the cosmic ray energy density declines toward the outer boundaries ($x = \pm\pi$) and shows some moderate variation inside the domain, but there is no pronounced correlation with the magnetic field. Indeed, the correlation between cosmic ray energy density and the local magnetic field strength is rather poor, as can be seen from a scatter plot. However, instead of a scatter plot where the points can become too dense we rather show in

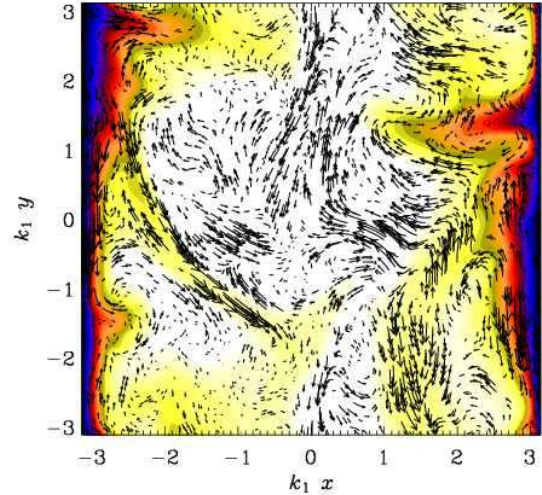


Figure 10. Cosmic ray energy density (colour/grey scale coded) and magnetic field vectors in a slice taken from a fully three-dimensional dynamo simulation.

Fig. 11 a two-dimensional probability density function which depicts essentially the point density in a grey/colour scale representation. As usual, the probability density function is normalized such that its integral is unity.

Apart from the fact that the confinement mechanisms discussed above are generally only marginally detectable, we must also note that the time dependence of the turbulence implies a finite life time of the magnetic structures and hence an even smaller degree of confinement. There are possibly other reasons as well. Padoan & Scalo (2005) have shown that, if the streaming velocity of cosmic rays is proportional to the Alfvén speed, the cosmic ray density is proportional to the square root of the gas density – independent of the magnetic field strength. However, in our simulations there is also no clear correlation between the magnetic field and the effective advection velocity of cosmic ray energy density.

The best correlation is between gas density and cosmic ray energy density, as shown in the form of a scatter plot or better a two-dimensional probability density function in Fig. 12. The well-pronounced anticorrelation of gas density and cosmic ray energy density is compatible with (statistical) pressure equilibrium within the domain. This is caused partly by the decline of cosmic ray pressure towards the boundaries. To maintain pressure equilibrium, the gas pressure and hence the gas density have to increase near the boundaries. However, even away from the boundary there is a clear anticorrelation between cosmic ray energy density and gas energy density, but it is combined with a simultaneous variation of the magnetic energy density as well. We can thus not verify the relation $e_c \sim \rho^{1/2}$, proposed by Padoan & Scalo (2005). In particular, we rather find an anticorrelation between the two quantities, as expected based on total pressure equilibrium. However, it is important to emphasize important differences in the two approaches: Padoan & Scalo (2005) do not include a source term as we do, and their assumption of the free streaming velocity being approximately the Alfvén speed is not well obeyed in our simulations. In fact, the cosmic ray streaming

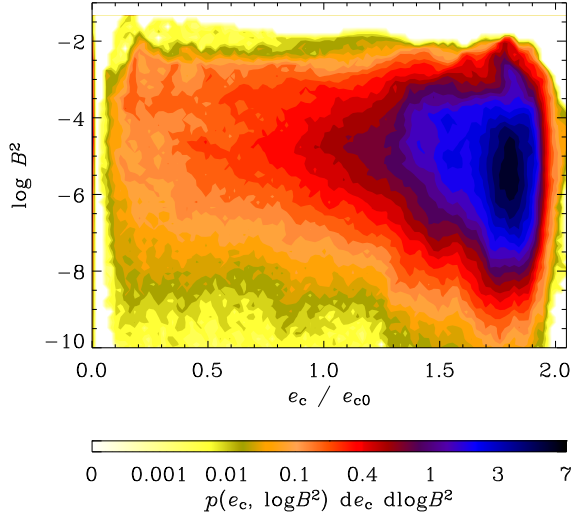


Figure 11. Two-dimensional histogram (or probability density function) of magnetic pressure and cosmic ray energy density. The correlation coefficient is only $r = -0.16$.

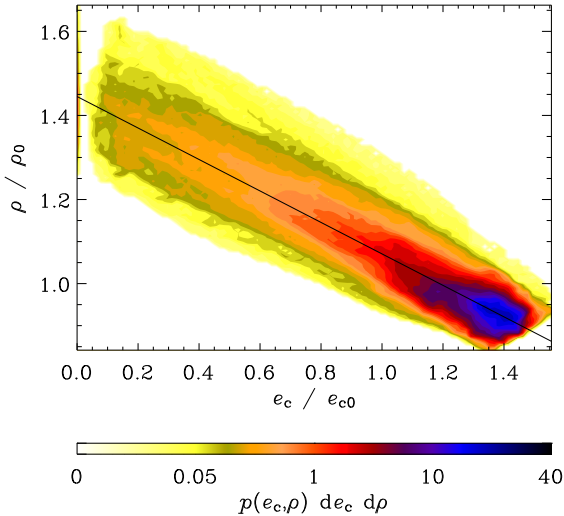


Figure 12. Two-dimensional histogram of gas density and cosmic ray energy density showing the anti-correlation between the two. Here, $e_{c0} = L_x^2 \tilde{Q}_c / K_{\parallel}$ is used to normalize e_c . The correlation coefficient is $r = -0.94$.

velocity can be a linear combination of the gas velocity and the Alfvén velocity (Skinging 1975)

5 CONCLUSION

The present results have shown that cosmic ray confinement is not easy to simulate in the diffusion approximation. Two possible mechanisms involving cosmic ray confinement have been investigated; the pressure from cosmic rays and their preferential diffusion along magnetic field lines. The former mechanism proves to be relatively inefficient: a localized enhancement of cosmic ray energy launches a wave of cosmic ray energy density that propagates outwards, but in practice

it does not lead to a significant outward transport of cosmic ray energy beyond the immediate vicinity of the original perturbation. The latter mechanism, which relies on preferential diffusion along field lines, is more effective in confining cosmic rays and it can, at least in principle, lead to an enhancement of cosmic ray energy density inside magnetic structures if there is an efficient removal of cosmic rays outside the magnetic structures. Here we have demonstrated that cosmic rays injected outside magnetic structures can be quickly transported close to the boundaries of the domain, if the (weak) field outside the structures is mostly randomly oriented. Once the cosmic rays have reached the boundaries, they can easily be lost from the domain.

The situation changes when the flow is turbulent. In that case the magnetic structures change in position and shape. Even if cosmic rays are confined at one time, they would easily appear “misplaced” at a later time when the flux tube has changed position. Only in the ideal case (no diffusion) and for weak fields (no Lorentz force) would both magnetic and cosmic ray structures be advected with the same speed, but this is not the case here. Examples where magnetic and cosmic ray structures appear to be misplaced have been seen in various slices similar to those shown in Fig. 10, where some of the structures are just next to each other, and yet they do not quite coincide in position.

The thickness of the magnetic structures found in the present simulations is typically of the resistive scale. While this is quite typical of many turbulence simulations (Brandenburg et al. 1995), it should be noted that one is often anticipating much thicker tube-like structures. This picture is usually motivated by analogy with the sun, where the sunspots are believed to be formed by flux tubes whose diameter would be related to that of sunspots (see, e.g., Schüssler 1980; D’Silva & Choudhuri 1993; Caligari et al. 1995). Sunspots would form when these flux tubes poke through the surface. However, this picture may not be true and sunspots may rather be an isolated surface phenomenon (see, e.g., Brandenburg 2005, for a recent discussion in the solar dynamo context). It may then be conceivable that also in galaxies the field is not really in the form of well defined tubes, but that it is much more diffuse and space-filling. In that case, cosmic ray-assisted magnetic buoyancy may not be an important factor. However, on the global scale of galaxies magnetic confinement is still likely to operate.

Our results suggest that a global equilibrium of cosmic ray energy, that is comparable to or even in excess of the thermal energy, can be established at relatively low cosmic ray injection rates. Here we have chosen a nondimensional injection rate of $\tilde{Q}_c = 0.01$. As discussed at the end of Sect. 2.2, even $\tilde{Q}_c = 1$ would still be about ten times below the rate of energy injection into the galaxy. This suggests that in a real galactic disc the losses of cosmic rays through the boundaries may be much more important. We have already discussed the issue that τ should perhaps be about ten times larger, but this would not be sufficient to explain the large discrepancy. Another aspect is that we have omitted lateral losses, but this too would not be sufficient. The effects of resolution have not really been assessed in the present work, but it is conceivable that higher resolution may allow the cosmic ray energy to stay more concentrated until cosmic rays can be released at the boundaries. Yet another important contributor is vertical gravitational stratification

which might facilitate additional losses through the Parker instability.

APPENDIX A: BOUNDEDNESS OF COSMIC RAY ENERGY DENSITY

In this section we show that, in a closed or periodic domain, $\max(e_c)$ can only decrease as a result of (tensorial) diffusion. This is useful for showing that the diverging behaviour of U_c does not produce a singularity in e_c ; cf. Sect. 2.2. In order to avoid interference from other effects, we assume that the evolution of e_c is only governed by diffusion, i.e.

$$\frac{\partial e_c}{\partial t} = \nabla_i (K_{ij} \nabla_j e_c). \quad (\text{A1})$$

Note also that $\max(e_c) = \langle e_c^n \rangle^{1/n}$ for $n \rightarrow \infty$. Here, angular brackets denote volume averages. Thus, we have

$$\begin{aligned} \frac{d}{dt} \langle e_c^n \rangle &= n \left\langle e_c^{n-1} \frac{\partial e_c}{\partial t} \right\rangle \\ &= n \left\langle e_c^{n-1} \nabla_i (K_{ij} \nabla_j e_c) \right\rangle \\ &= -n(n-1) \left\langle e_c^{n-2} K_{ij} (\nabla_i e_c) (\nabla_j e_c) \right\rangle \\ &\leq 0, \end{aligned} \quad (\text{A2})$$

where we have used integration by parts. The last inequality assumes that the diffusion tensor is positive definite, which is true in our case, because

$$K_{ij} (\nabla_i e_c) (\nabla_j e_c) = (K_{\parallel} - K_{\perp}) (\hat{\mathbf{B}} \cdot \nabla e_c)^2 + K_{\perp} (\nabla e_c)^2 \quad (\text{A3})$$

is positive. Therefore, $\max(e_c)$ must decrease with time.

APPENDIX B: THE FORCING FUNCTION

For completeness we specify here the forcing function used in the present paper². It is defined as

$$\mathbf{f}(\mathbf{x}, t) = \text{Re}\{N \mathbf{f}_{\mathbf{k}(t)} \exp[i\mathbf{k}(t) \cdot \mathbf{x} + i\phi(t)]\}, \quad (\text{B1})$$

where \mathbf{x} is the position vector. The wavevector $\mathbf{k}(t)$ and the random phase $-\pi < \phi(t) \leq \pi$ change at every time step, so $\mathbf{f}(\mathbf{x}, t)$ is δ -correlated in time. For the time-integrated forcing function to be independent of the length of the time step δt , the normalization factor N has to be proportional to $\delta t^{-1/2}$. On dimensional grounds it is chosen to be $N = f_0 \rho_0 c_s (|\mathbf{k}| c_s / \delta t)^{1/2}$, where f_0 is a nondimensional forcing amplitude. The value of the coefficient f_0 is chosen such that the maximum Mach number stays below about 0.5; in practice this means $f_0 = 0.01 \dots 0.05$, depending on the average forcing wavenumber. At each timestep we select randomly one of many possible wavevectors in a certain range around a given forcing wavenumber. The average wavenumber is referred to as k_f . Two different wavenumber intervals are considered: 1...2 for $k_f = 1.5$ and 4.5...5.5 for $k_f = 5$. We force the system with transverse helical waves,

$$\mathbf{f}_{\mathbf{k}} = \mathbf{R} \cdot \mathbf{f}_{\mathbf{k}}^{(\text{nohel})} \quad \text{with} \quad R_{ij} = \frac{\delta_{ij} - i\sigma \epsilon_{ijk} \hat{k}_k}{\sqrt{1 + \sigma^2}}, \quad (\text{B2})$$

² This forcing function was also used by Brandenburg (2001), but in his Eq. (5) the factor 2 in the denominator should have been replaced by $\sqrt{2}$ for a proper normalization.

where $\sigma = 1$ for positive helicity of the forcing function,

$$\mathbf{f}_{\mathbf{k}}^{(\text{nohel})} = (\mathbf{k} \times \hat{\mathbf{e}}) / \sqrt{\mathbf{k}^2 - (\mathbf{k} \cdot \hat{\mathbf{e}})^2}, \quad (\text{B3})$$

is a non-helical forcing function, and $\hat{\mathbf{e}}$ is an arbitrary unit vector not aligned with \mathbf{k} ; note that $|\mathbf{f}_{\mathbf{k}}|^2 = 1$.

ACKNOWLEDGEMENTS

We are grateful to M. Hanasz for useful discussions. This work was supported by PPARC grants PPA/S/S/2000/02975A, PPA/S/S2002/03473 and PPA/G/S/2000/00528. We acknowledge the Danish Center for Scientific Computing for granting time on the Horseshoe cluster. APS, AJM and AS are grateful to Nordita for financial support and hospitality.

REFERENCES

- Berezinskii, V. S., Bulanov, S. V., Dogiel, V. A., Ginzburg, V. L., & Ptuskin, V. S. 1990, *Astrophysics of Cosmic Rays* (V. L. Ginzburg, ed.), Amsterdam, North-Holland
- Blackman, E. G., & Field, G. B. 2003, *Phys. Fluids*, 15, L73
- Barge, P., & Sommeria, J. 1995, *A&A*, 295, L1
- Brandenburg, A. 2001, *ApJ*, 550, 824
- Brandenburg, A. 2005, *ApJ*, 625, 539
- Brandenburg, A., & Dobler, W. 2001, *A&A*, 369, 329
- Brandenburg, A., Käpylä, P., & Mohammed, A. 2004, *Phys. Fluids*, 16, 1020
- Brandenburg, A., Procaccia, I., & Segel, D. 1995, *Phys. Plasmas*, 2, 1148
- Caligari, P., Moreno-Inertis, F., & Schüssler, M. 1995, *ApJ*, 441, 886
- D'Silva, S., & Choudhuri, A. R. 1993, *A&A*, 272, 621
- Drury, L. O'C., & Völk, J. H. 1981, *ApJ*, 248, 344
- Elperin, T., Kleeorin, N., & Rogachevskii, I. 1996, *Phys. Rev. Lett.*, 77, 5373
- Elperin, T., Kleeorin, N., & Rogachevskii, I. 1997, *Phys. Rev. E*, 55, 2713
- Farmer, A. J., & Goldreich, P. 2004, *ApJ*, 604, 671
- Felice, G. M., & Kulsrud, R. M. 2001, *ApJ*, 553, 198
- Jun, B.-I., Clarke, D. A., & Norman, M. L. 1994, *ApJ*, 429, 748
- Hanasz, M. & Lesch, H. 2003, *A&A*, 412, 331
- Hanasz, M., Kowal, G., Otmianowska-Mazur, K., & Lesch, H. 2004, *ApJ*, 605, L33
- Haugen, N. E. L., Brandenburg, A., & Dobler, W. 2004, *Phys. Rev. E*, 70, 016308
- Johansen, A., Andersen, A. C., & Brandenburg, A. 2004, *A&A*, 417, 361
- Hodgson, L. S. & Brandenburg, A. 1998, *A&A*, 330, 1169
- Kang, H., & Jones, T. W. 1990, *ApJ*, 353, 149
- Korpi, M. J., Brandenburg, A., Shukurov, A., et al. 1999, *ApJ*, 514, L99
- Kóta, F., & Jokipii, J. R. 2000, *ApJ*, 531, 1067
- Krause, F. 1972, *AN*, 294, 83
- Krause, F., & Rädler, K.-H. 1980, *Mean-Field Magnetohydrodynamics and Dynamo Theory* (Akademie-Verlag, Berlin; also Pergamon Press, Oxford)

- Landau, L. D., & Lifshitz, E. M. 1987, Fluid Dynamics
(2nd Edition, Pergamon Press, Oxford)
- Moss, D., Shukurov, A., & Sokoloff, D. 1999, A&A, 343,
120
- Padoan, P., & Scalo, J. 2005, ApJ, 624, L97
- Parker, E. N. 1966, ApJ, 145, 811
- Parker, E. N. 1992, ApJ, 401, 137
- Ryu, D., Kim, J., Hong, S. S., & Jones, T. W. 2003, ApJ,
589, 338
- Schüssler, M. 1980, Nat, 288, 150
- Skilling, J. 1975, MNRAS, 172, 557
- Strong, A. W. & Moskalenko, I. V. 1998, ApJ, 509, 212
- Yousef, T. A., Brandenburg, A., & Rüdiger, G. 2003, A&A,
411, 321
- Zeldovich, Ya. B., Ruzmaikin, A. A., & Sokoloff, D. D.
1990, The Almighty Chance (World Scientific, Singapore)